HHS Public Access

Author manuscript

Neurotoxicology. Author manuscript; available in PMC 2018 January 01.

Published in final edited form as:

Neurotoxicology. 2017 January ; 58: 11–22. doi:10.1016/j.neuro.2016.10.015.

Influence of Tetramethylenedisulfotetramine on Synchronous Calcium Oscillations at Distinct Developmental Stages of Hippocampal Neuronal Cultures

Zhengyu Cao[1,2,*], **Jian Xu**[1], **Susan Hulsizer**[2], **Yanjun Cui**[2], **Yao Dong**[2], and **Isaac N. Pessah**[2,*]

[1]State Key Laboratory of Natural Medicines & Jiangsu Provincial Key Laboratory for TCM Evaluation and Translational Development, China Pharmaceutical University, Nanjing, P.R. China, 211198

[2]Department of Molecular Biosciences, School of Veterinary Medicine, University of California, Davis, 95616

Abstract

The spatial and temporal patterns of spontaneous synchronous Ca^{2+} oscillations (SCOs) regulate physiological pathways that influence neuronal development, excitability, and health. Hippocampal neuronal cultures (HN) and neuron/glia co-cultures (HNG) produced from neonatal mice were loaded with Fluo-4/AM and SCOs recorded in real-time using a Fluorescence Imaging Plate Reader at different developmental stages *in vitro*. HNG showed an earlier onset of SCOs, with low amplitude and low frequency SCOs at 4 days *in vitro* (DIV), whereas HN were quiescent at this point. SCO amplitude peaked at 9 DIV for both cultures. SCO network frequency peaked at 12 DIV in HN, whereas in HNG the frequency peaked at 6 DIV. SCO patterns were associated with the temporal development of neuronal networks and their ratio of glutamatergic to GABAergic markers of excitatory/inhibitory balance. HN and HNG exhibited differential responses to the convulsant tetramethylenedisulfotetramine (TETS) and were highly dependent on DIV. In HN, TETS triggered an acute rise of intracellular Ca^{2+} (Phase I response) only in 14 DIV and a sustained decrease of SCO frequency with increased amplitude (Phase II response) at all developmental stages. In HNG, TETS decreased the SCO frequency and increased the amplitude at 6 and 14 but not 9 DIV. There was no acute Ca^{2+} rise (Phase I response) in any age of HNG tested with TETS. These data demonstrated the importance of glia and developmental stage in modulating neuronal responses to TETS. Our results illustrate the applicability of the model for

[*]***Correspondence:*** **Zhengyu Cao, Ph.D.**, State Key Laboratory of Natural Medicines & Jiangsu Provincial Key Laboratory for TCM Evaluation and Translational Development, China Pharmaceutical University, Nanjing, P.R. China, 211198, zycao1999@hotmail.com, Tel: 86-25-86185157, Fax: 86-25-86185158; **Isaac N. Pessah, Ph.D.**, Department of Molecular Biosciences, School of Veterinary Medicine, University of California, Davis, 95616, inpessah@ucdavis.edu, Tel: 530-752-6696.

Conflict of interest

The authors declare no conflicts of interest.

investigating how caged convulsants elicit abnormal network activity during the development of HN and HNG cultures *in vitro*.

Keywords

Tetramethylenedisulfotetramine; Hippocampal neuronal network; Calcium oscillations

Introduction

Neural development is a highly regulated process that involves activity-dependent and activity-independent mechanisms. Primary cultures of embryonic hippocampal neurons predominantly contain pyramidal glutamatergic neurons together with a low percentage of inhibitory GABAergic cells (Bateup et al., 2013, Puranam et al., 2015). Within the first week in culture axonal length and dendritic complexity increase as neuronal networks form and stabilize synapses. Spontaneous neurotransmission that promotes maturation of neuronal circuits *in vitro* exhibit membrane electrical activity (electrical spike activity; ESA) and spontaneous Ca^{2+} oscillations (SCOs), two fundamentally interrelated physiological signals that are essential for normal neuronal network development (Clause et al., 2014). Such spontaneous activity controls the pattern of a number of genes that regulate the rate of neuronal cell migration (Jabba et al., 2010), patterning of synaptic connections (Spitzer, 2006, Kerschensteiner et al., 2009), and neuronal plasticity (Saneyoshi et al., 2010, Basu and Siegelbaum, 2015). Spatial and temporal abnormalities in the frequency and amplitude of the cytosolic SCO and/or ESA activity can not only impact physiological processes of individual neurons, but also pathophysiological sequelae that may alter their interactions with glia, which in turn influences the architecture and functional integrity of the networks they form.

Tetramethylenedisulfotetramine (TETS) is a rodenticide which was banned worldwide in the early 1990s (Whitlow et al., 2005). However, several accidental and intentional poisonings have been reported since the ban, predominantly in China (Cao et al., 2012a), but also in the United States (Barrueto et al., 2003). Administration of TETS to animals produces convulsive activity, which resembles those produced by other $GABA_A$ receptor blockers such as picrotoxin (PTX) (Zolkowska et al., 2012, Flannery et al., 2015, Shakarjian et al., 2015). The specificity of TETS in blocking $GABA_A$ receptors is supported by binding experiments. TETS was shown to inhibit [^{35}S]t-butylbicyclophosphorothionate ([^{35}S]TBPS) binding to brain membranes (Squires et al., 1983) and suppress GABA-stimulated Cl^- uptake in membrane vesicles prepared from both rat and human brains (Ratra et al., 2001). In addition, the binding of [^{14}C]TETS to rat brain membranes was suppressed by an array of $GABA_A$ receptor modulators (Zhao et al., 2014). Recently, TETS was shown to bind to a site somewhat distinct from either that occupied by [^{35}S]TBPS or [^{3}H]ethynylbicycloorthobenzoate ([^{3}H]EBOB) which have been mapped for cage convulsants (Zhao et al., 2014).

Radioligand-receptor binding analyses have demonstrated that TETS and PTX display comparable affinity on $GABA_A$ receptors prepared from rat brain as well as the $GABA_A$

receptors composed with α1β3γ2 subunits (Squires et al., 1983, Ratra et al., 2001). Recent evidence with [^{14}C]TETS indicates that the binding sites for TETS and PTX are distinct, and may preferentially interact with distinct $GABA_A$ receptor subunits (Zhao et al., 2014). When administrated orally, TETS was 40-times more potent than picrotoxin although the estimated blood/brain concentration ratio was comparable for TETS (0.2) and picrotoxin (0.35) (Zolkowska et al., 2012, Flannery et al., 2015, Shakarjian et al., 2015). Thus the molecular mechanisms responsible for the acute seizurogenic potency of TETS remain unclear, and its neuropathological sequelae appear to have a neuroinflammatory component (Zolkowska et al., 2012).

Recently we developed a rapid throughput method to quantitatively measure how seizurogenic chemicals alter Ca^{2+} dynamics in enriched hippocampal neuronal cultures (Cao et al., 2015). Importantly, seizurogenic chemicals that engage distinct receptor targets were found to produce distinct changes in Ca^{2+} dynamics and SCO patterns. Analysis of *in vitro* SCO patterns may serve not only as valuable rapid screening tool for identifying and classifying excitotoxicity of potential seizurogenic agents, but may also serve as a valuable means of high throughput discovery of anticonvulsants (Cao et al 2012a; Brunn et al., 2015). In this regard, new and innovative approaches and analytical tools are emerging for measurement and analysis of SCO patterns produced by dissociated neuronal networks and intact brain slices(Hongo et al., 2015, Jang and Nam, 2015, Patel et al., 2015). Such approaches also lend themselves for studies of developmental neurotoxicants (Cao et al., 2014b) and those that promote neurodegeneration.

The chemicals known to block $GABA_A$ receptors have been investigated in cultured hippocampal neuronal models but results are somewhat contradictory. In rat primary cultured hippocampal neurons grown with a glial monolayer, the addition of 100 μM PTX was without obvious effect on SCO frequency and amplitude at 12–14 DIV (Bacci et al., 1999). In contrast murine hippocampal cultures with a very low density of glial cells responded vigorously to PTX (100 μM) and bicuculline (100 μM) at 14 DIV, with both compounds altering SCO amplitude and frequency as well as electric spike activity in manners similar to those elicited by TETS (Cao et al., 2012a, Cao et al., 2012b). These data suggest that the presence of glia in hippocampal neuronal cultures influences hippocampal neuronal network formation and function, as revealed through their sensitivity to $GABA_A$ receptor blockade.

Here, we use rapid throughput Fluorescence Imaging Plate Reader (FLIPR®) to systematically investigate neuronal SCOs patterns at distinct developmental stages in two types of murine cultures: *(1)* Those enriched in hippocampal neurons and deficient in glia (HN), and *(2)* Hippocampal neuron/glia co-cultures (HNG). HN and HNG display distinct SCO patterns during *in vitro* development and different expression of glutamatergic (vesicular glutamate transporter 1, vGLUT1)/GABAergic (vesicular GABA transporter, vGAT) markers of excitatory/inhibitory balance. Importantly, HN and HNG networks exhibit differential responses to acute challenge with TETS that are dependent on the developmental stage of the cultures. These data demonstrate the importance of astrocytes and developmental stage in modulating neuronal SCO patterns with TETS. Our results illustrate the applicability of the model to identify caged convulsants.

Materials and methods

Materials

Fetal bovine serum and soybean trypsin inhibitor were obtained from Atlanta Biologicals (Norcross, GA). DNase I, Hoechst 33342, poly-L-lysine, chemical reagents, and cytosine β-D-arabinofuranoside (ARA-C) were from Sigma-Aldrich (St. Louis, MO). Anti-vGAT (vesicular GABA transporter), anti-vGLUT1 (vesicular glutamate transporter 1) and anti-MAP-2B (microtubule-associated protein 2B) anti-bodies were from Synaptic Systems (Goettingen, Germany) and anti-GFAP (glial fibrillary acidic protein) and anti-β-actin antibodies were purchased from Cell Signaling Technology (Danvers, MA). Anti-$GABA_AR$ α5 subunit antibody was from Abcam Inc. (Cambridge, MA). Anti-$GABA_AR$ γ2 subunit antibody was from EMD Millipore (Billerica, MA). The BCA kit, Ca^{2+} fluorescence dye Fluo-4/AM, Neurobasal medium, nitrocellulose membrane, Alexa Fluor 488-conjugated goat anti-guinea pig and Alexa Fluor-568-conjugated goat anti-mouse antibodies were purchased from Life Technology (Grand Island, NY). Protein markers and 4–15% gradient SDS-PAGE gels were from BioRad Laboratory (Hercules, CA). Protease inhibitor cocktail was from Roche Diagnostics (Branchburg, NJ). NS21 serum-free supplement was formulated in the laboratory as previously described (Chen et al., 2008), stored in aliquots at −80 °C. Tetramethylenedisulfotetramine (TETS) was synthesized as described previously and was determined to be above 99% purity (Zolkowska et al., 2012).

Primary cultures of hippocampal neurons

Animals were treated humanely and with regard for alleviation of suffering according to protocols approved by the Institutional Animal Care and Use Committee of the University of California, Davis. The C57BL/6J mouse pups at postnatal day 1–2 were decapitated and the hippocampi were dissected and collected in cold dissection buffer [in mM: NaCl 124, KCl 5.4, NaH_2PO_4 1.0, D-glucose 14.4, HEPES 25, $MgCl_2$ 3.2, BSA, 3 mg/ml, pH 7.4]. After stripping the meninges, the hippocampi were digested with a 0.25% trypsin solution (0.25 ml/hippocampus) for 25 min at 37 °C. The cells were then dissociated by trituration using a glass Pasteur pipette and sedimented in dissection buffer containing soybean trypsin inhibitor (0.2 mg/ml) and DNase I (25 μg/ml). After centrifugation at 180 g for 5 min, the cells were resuspended in Neurobasal complete medium [Neurobasal medium supplemented with NS21 (2%, v/v), 0.5 mM L-glutamine, 10 mM HEPES] with 5% fetal bovine serum. Dissociated hippocampal cells were plated onto poly-L-lysine (0.5 mg/ml) pre-coated clear-bottom, black wall, 96-well imaging plates (BD, Franklin Lakes, NJ) or 6-well plates (Corning Inc., Corning, NY) at densities of 7.5×10^4 cells/well and 1.8×10^6 cells/well, respectively. To prevent the glia dividing in enriched hippocampal neuron cultures (HN), after plating the cells for 24–36 h, the DNA synthesis inhibitor cytosine β-D-arabinofuranoside (ARA-C, dissolved in Neurobasal complete medium) was added at 10 μM (Dravid and Murray, 2004, George et al., 2009). The mixed neuron/glia co-cultures (HNG) were not exposed to ARA-C. The medium was changed every three days starting at 6 DIV by replacing half the volume of the media with fresh Neurobasal complete medium. The cultures were maintained at 37 °C with 5% CO_2 and 95% humidity until used.

Immunocytochemistry

The cultured cells in 96-well plates at 6, 9, 12 DIV were fixed with 4% paraformaldehyde for 20 min and then permeabilized with 0.25% triton x-100 for 15 min followed by 1 h blocking with PBS containing 10% BSA and 1% goat serum. After incubation with anti-MAP-2B (1:1000) and anti-GFAP (1:500) antibodies at 4 °C overnight in PBS containing 1% goat serum, cells were then incubated with Alexa Fluor 488-conjugated goat anti-guinea pig (1:500) and Alexa Fluor-568-conjugated goat anti-mouse (1:500) secondary antibodies for 1 h at room temperature. After washing, a concentration of 0.2 μg/ml Hoechst 33342 was added to stain the nuclei. Pictures were digitized using an ImageXpress High Content Imaging System (Molecular Devices, Sunnyvale, CA) with a 10× objective under DAPI, FITC, and TXRED filters. Nine adjacent sites (3×3) which cover ~60% of the center surface area were digitized from each well. The total fluorescence intensity of each image was analyzed using MetaXpress software (Molecular Devices, Sunnyvale, CA).

Measurement of synchronous Ca^{2+} oscillations (SCOs)

HN and HNG cultures in 96-well plates were withdrawn from the culture incubator at 4, 6, 9, 12, 15 DIV to investigate the basal developmental patterns of SCO evens and how they were modified by TETS using Fluorescent Imaging Plate Reader (FLIPR, Molecular Devices, Sunnyvale, CA). This method permitted a high temporal resolution (every half second) recording of internal Ca^{2+} concentration to reveal SCO dynamics in parallel across 96 wells before and after exposure to TETS (Cao et al., 2015). After aspirating the medium, a volume of 100 μl of Locke's buffer (in mM: 8.6 HEPES, 5.6 KCl, 154 NaCl, 5.6 glucose, 1.0 $MgCl_2$, 2.3 $CaCl_2$, and 0.1 glycine, pH 7.4) containing Fluo-4 (4 μM) and BSA (1 mg/ml) was added to each well immediately and incubated in a 37 °C CO_2 incubator for 1h. The extracellular Fluo-4 was removed by adding and removing 200 μl Locke's buffer repeated for 5 times. The final volume of each well was adjusted to 175 μl. The plate was then transferred to the FLIPR chamber which was pre-set to be 37 °C. Cells were excited at 488 nm, and Ca^{2+}-bound Fluo-4 emission was recorded at 535 nm. Baseline recording were acquired at a sampling rate of 0.5 s^{-1} for 3 min followed by an addition of TETS (25 μl in Locke's buffer, 8× final concentration) using a programmable 96-channel robotic pipetting system and the fluorescent signals was recorded for an additional 30 min. FLIPR measures the Ca^{2+} dynamics from a center area of each well therefore represents the average Ca^{2+} signals from a population of cells. The SCO activity was dependent on the N-methyl-D-Aspartate (NMDA) receptor. To achieve the NMDA receptor function, the NMDA receptor co-agonist, glycine was included in the Locke's buffer at a saturation concentration (100 μM). To quantify the Ca^{2+} signals, data were presented as $(F-F_0)/F_0$ ($\Delta F/F_0$) where F is the fluorescent signal at different time points whereas F_0 is the average of the basal fluorescence from an initial five data points. An increase of $\Delta F/F_0 \geqslant 0.1$ unit was considered to be an SCO event.

Western blot

The cells cultured in 6-well plates were washed 2× with ice-cold PBS then 150 μl of ice-cold lysis buffer (in mM: Tris 50, NaCl 50, EDTA 2, sodium pyrophosphate 2.5, sodium orthovanadate 1, phenylmethylsulfonyl fluoride 1, containing protease inhibitor cocktail and

1% NP-40) was added to each well and incubated for 10 min at 4 °C. Cell lysates then underwent sonification and were centrifuged at 16,000 g for 10 min at 4 °C. The supernatant obtained after centrifugation of the lysate was assayed for protein concentration using a BCA kit (Life Technology, Grand Island, NY). Equal amounts of protein were mixed with the 4× Laemmli SDS sample buffer (BioRad, Hercules, CA) and boiled for 5 min. An equal amount (15 μg) of protein sample was then loaded onto the well of a 4–15% gradient SDS–PAGE gels (15-well). The samples were separated by electrophoresis with a constant voltage of +145 V for 1 h. The protein markers were used to determine the molecular weights of the bands. After electrophoresis, the protein samples were transferred to a nitrocellulose membrane (0.2 μm) by electroblotting under a constant voltage of +102 V for 75 min. The membranes were then blocked with Odyssey Blocking Buffer (LI-COR Biotechnology, Lincoln, NE) containing 0.1% Tween-20 for 1 h at room temperature. After blocking, membranes were incubated overnight at 4°C with primary anti-bodies (anti-$GABA_A$ γ2, 1:1000; anti-$GABA_A$ α5, 1:1000; anti-β-actin, 1:5000; anti-vGAT, 1:1000 or anti-vGLUT1, 1:1000) diluted in Odyssey Blocking Buffer. The blots were washed for four times with PBS +0.1% Tween-20 and incubated with the IRDye (700CW or 800CW)-labeled goat-anti-mouse or goat-anti-rabbit secondary antibodies (1:5,000; LI-COR Biotechnology, Lincoln, NE) diluted in Odyssey Blocking Buffer for 1 h at room temperature. After washing with PBS+0.1% Tween-20 for five times, the membrane was scanned with the LI-COR Odyssey Infrared Imaging System (LI-COR Biotechnology, Lincoln, NE) under the western blot mode. Densitometry was quantified using the LI-COR Odyssey Infrared Imaging System application software 2.1. Membranes were stripped with NewBlot Nitro Stripping Buffer (LI-COR Biotechnology, Lincoln, NE) and re-blotted for further analysis of additional proteins.

Data analysis

Total MAP-2B and GFAP fluorescence intensities of each image were quantified using MetaXpress software (Molecular Devices, Sunnyvale, CA). The graphing of immunochemistry fluorescence intensity and western blot densitometry data were performed using GraphPad Prism software (Version 5.0, GraphPad Software Inc., San Diego, CA). Statistical significance analysis between different culture DIVs was performed by one-way ANOVA followed by *post hoc* Dunnett Test (GraphPad, Version 5.0, Graphpad Software Inc., San Diego, CA). A p value below 0.05 was considered to be statistically significant. The FLIPR calcium data were exported to an excel sheet and the time-response relationship figures were generated using GraphPad Prism software (Version 5.0, GraphPad Software Inc., San Diego, CA). The SCO frequency and amplitude were quantified by Origin software (Ver 9.1, Origin Lab, Northampton, MA). The TETS frequency and amplitude response (Phase II response) was obtained from an epoch of 10 min after addition of TETS for 20 min. The TETS acute increase in intracellular Ca^{2+} concentration was calculated by GraphPad Prism software in a 10-min time period right after addition of TETS. The TETS response was normalized to the vehicle control (0.1% DMSO). The concentration-response relationship curves were fit by a three parameter non-linear equation using GraphPad Prism software (Version 5.0, GraphPad Software Inc., San Diego, CA).

Results

HN and HNG cultures display divergent developmental trajectories and temporal patterns of SCOs

Immunocytochemical staining with neuronal marker MAP-2B showed that at 6 DIV, hippocampal neurons cultured in 96-well plates at an initial density of 75,000 cells/well displayed extensive dendritic network connectivity both in enriched neuronal cultures (HN) and neuron/glia mixed co-cultures (HNG) that increased their complexity with age in culture (Fig. 1A&B, green channel). In the cultures exposed to 10 μM ARA-C 24–36 h post plating, the percentage of glial cells (GFAP positive, red channel) was less than 5% of the total cell count (Fig. 1A, left panel). In contrast, a high percentage of GFAP positive glia existed in the culture without ARA-C post-treatment, which modestly increased with age during the timeframe of this study (Fig. 1A right panel, Fig. 1C).

Consistent with our previous report (Cao et al., 2015), we found that HN neurons produced characteristic patterns of spontaneous synchronous Ca^{2+} oscillations (SCOs) as they developed network complexity (Fig. 2A&C). HN cultures at 4 DIV displayed infrequent SCOs with small amplitude (Fig. 2A, top trace). By 6 DIV, SCOs became pronounced and displayed regular periodicity and similar amplitudes across the experimental recording that lasted at least 30 minutes (Fig. 2A, second trace). At 9 DIV, average SCO amplitude and frequency continued to increase (Fig. 2A, third trace). At this time, SCOs displayed larger variability in amplitude. By 12 DIV, SCO frequency continued to increase while the amplitude declined (Fig. 2A, fourth trace). At 16 DIV, SCO amplitude was more heterogeneous and continued to decline (Fig. 2A, fifth trace). Summary data for n=3 independent HN cultures are summarized in panel 2C.

The HNG culture also displayed a developmental change of SCO patterns. HNG cultures at 4 DIV displayed lower amplitude but more frequent SCO events compared to 4 DIV HN cultures (Fig. 2B, top trace). At 6 DIV, SCOs in HNG became more pronounced with regular periodicity and more homogeneous amplitudes across the recording period (Fig. 2B, second trace). By 9 DIV, HNG cultures displayed higher SCO amplitudes, whereas their frequency declined (Fig. 2B, third trace). At 12 DIV, the amplitude of SCO started to decline whereas the frequency was increased compared to that of 9 DIV (Fig. 2B, fourth trace). It should be noted that although five batches of HNG cultures displayed consistent developmental patterns of SCOs until 9 DIV, 2 out of 5 cultures displayed a very high frequency (HF) low amplitude events commencing greater than 12 DIV which was not resolved by FLIPR (Fig. 2B, fifth and seventh traces). Since the amplitude of SCOs from these traces was smaller than 0.1 units ($\Delta F/F_0$), we didn't quantify the frequency and amplitude of these high frequent SCOs. Thus, as the neuronal network gained morphological complexity (Fig. 1), SCOs ran a course from low amplitude, low frequency events, to high amplitude, intermediate frequency events and later intermediate amplitude, high frequency oscillations (Fig. 2). TTX suppressed basal SCOs in HN cultures suggesting that these SCOs were dependent on spontaneous action potentials (Supplemental Fig. 1).

Developmental changes of vGLUT and vGAT in HN cultured neurons

The vesicular glutamate (Glu) and GABA transporters (vGLUT and vGAT) are expressed primarily in excitatory and inhibitory neurons respectively (Balschun et al., 2010), and are responsible for the uptake of Glu and GABA into presynaptic vesicles (McIntire et al., 1997, Bellocchio et al., 2000). Disruption in the balance between an excitatory and inhibitory transmission has been shown to influence overall neuronal activity (Dravid and Murray, 2004, Koga et al., 2010). We therefore investigated the vGLUT1 and vGAT expression levels in HN and HNG cultures at different stages of *in vitro* development using western blot analysis (Fig 3A and 3B respectively). In both HN and HNG cultures, the expression levels of vGAT were consistent through the *in vitro* developmental window examined in this study (Fig. 3A–C). However, the vGLUT1 expression levels significantly increased as the HN and HNG cultures matured (Fig. 3A, B&D). The ratio of vGAT/vGLUT1 decreased with maturation of HN and HNG cultures, suggesting that during the developmental window investigated, the excitability of the entire neuronal network increased (Fig. 3E).

Expression levels of $GABA_A$ receptors during in vitro neuronal development

The $GABA_A$ receptors function as the major inhibitory inputs in HN and HNG neuronal networks formed *in vitro*. We therefore determined whether expression patterns of $GABA_A$ receptors $\gamma 2$ (synaptic) and $\alpha 5$ subunits differ as HN and HNG cultures mature using western blot analysis. The expression levels of the $\alpha 5$ subunit continued to increase as the HN cultures matured, whereas it remained unaltered in HNG cultures during developmental window investigated (Fig. 4A–C). In contrast, expression levels of the $GABA_A$ $\gamma 2$ subunit in HN and HNG cultures did not significantly change during developmental window investigated (Fig. 4A, B &D).

Neuronal responses to TETS are altered by network maturity and the presence of glia

When HN cultures were challenged with TETS at 6 DIV, they responded with concentration-dependent reduction of mean SCO frequency with an IC_{50} value of 0.22 μM (0.12–0.43 μM, 95% CI) and a maximal inhibition of 51.7% (43.5%–59.8%, 95% CI) of basal SCO frequency (Fig. 5A&C, Table 1). TETS also increased the mean SCO amplitude with an EC_{50} value of 0.56 μM (0.27–1.36 μM, 95% CI) (Fig. 5A&D, Table 1). In 6 DIV HNG cultures, addition of TETS produced a concentration-dependent reduction on the SCO frequency with IC_{50} value of 0.33 μM [0.08–1.43 μM, 95% Confidence Intervals (95% CI)] and a maximal inhibition of 49.6% (30.0%–69.3%, 95% CI) of basal SCO frequency (Fig. 5B&C, Table 1). TETS also slightly increased the mean SCO amplitude with an EC_{50} value of 0.56 μM (0.27–1.36 μM, 95% CI) and a maximal increase of 26.6% of basal SCO amplitude (18.0–35.2%) (95% CI, Fig. 5B&D, Table 1). Compared to the TETS response measured in HNG cultures at 6 DIV, the maximal increase in the mean SCO amplitude was much greater in HN cultures reaching 70.5% (47.0%–93.9% μM, 95% CI) increase over baseline (Fig 5D).

The responses to TETS on 9 DIV were dramatically different between HN and HNG cultures. HN cultures challenged with TETS at 9 DIV produced a robust reduction in the SCO frequency with an IC_{50} value of 0.24 μM (0.16–0.38 μM, 95% CI) and a maximal diminution of 65.8% (56.5%–75.4%, 95% CI) (Fig. 6A&C). TETS also dramatically

increased mean SCO amplitude with an EC_{50} value of 0.37 μM (0.15–0.96 μM, 95% CI) and a maximal increase of 174% (128%–221%, 95%CI) over baseline (Fig. 6A&D). In contrast, exposure of HNG cultures to TETS on 9 DIV neither altered the basal SCO frequency nor the mean amplitude at the concentrations tested (<10 μM) (Fig. 6B–D).

HN cultures exposed to TETS on 14 DIV elicited more profound changes on Ca^{2+} dynamics. TETS at concentrations (≥0.3μM) produced an acute sustained intracellular Ca^{2+} increase, which recovered slowly (Phase I response) (Fig. 7A). The integrated Ca^{2+} signal (area under curve, AUC) exhibited a concentration-dependent increase, with an EC_{50} value of 0.51 μM (0.39–0.67 μM, 95% CI) and a maximal response of 672% (AUC, 612%–831%) of control (Fig. 7C, Table 1). TETS also produced steady state decrease (Phase II frequency response) in the SCO frequency with an IC_{50} value of 0.30 μM (0.16–0.54 μM; 95% CI) and 65.5% (53.8%–77.3%, 95% CI) maximal inhibition (Fig. 7D, Table 1). Along with the decreased SCO frequency, TETS also increased mean SCO amplitude (Phase II amplitude response) with an EC_{50} value of 0.73 μM (0.64–0.83 μM, 95% CI) and an 893% (853%–933%, 95%CI) maximal increase (Fig. 7E, Table 1). The observed TETS response on HN cultures at 14 DIV is consistent with previous studies (Cao et al., 2012a, Bruun et al., 2015). By comparison, HNG culture at 14 DIV responded to TETS challenge in a manner similar to that observed on 6 DIV (Fig. 7B). TETS suppressed the SCO frequency with an IC_{50} value of 0.80 μM (0.29–2.10 μM, 95% CI) and a maximal reduction of 50.2% (Fig. 7D, Table 1). TETS also increased mean SCO amplitude with an EC_{50} value of 1.29 μM (0.75–2.30 μM, 95% CI) and a maximal increase of 83.3% (63.2%–103.3%, 95%CI) over baseline (Fig. 7E, Table 1).

Picrotoxin and TETS elicit similar changes in Ca^{2+} dynamics

Similar to Phase I response produced by TETS in 14 DIV HN, acute challenge with PTX elicited an acute Phase I-like Ca^{2+} response that was concentration-dependent with an EC_{50} value of 0.92 μM (0.73–1.15 μM, 95% CI) and maximal AUC of 747.3% (647.7–817.9%, 95% CI) of control in HN cultures at 14 DIV (Fig. 8A&B). PTX also caused a concentration-dependent decrease in SCO frequency with an IC_{50} value of 0.68 μM (0.59–0.79 μM, 95% CI) and a maximal reduction of 68.3% (51.0–85.0%, 95% CI) similar to TETS (Fig. 8C). Coincident with the reduction in the frequency, PTX increased mean SCO amplitude with an EC_{50} value of 0.34 μM (0.13–0.89 μM, 95% CI) and a maximal increase of 962% of control (912–1012%, 95%CI) (Fig. 8D).

Discussion

SCOs represent a common feature of developing mammalian neurons, both *in situ* (Bando et al., 2016), and in primary cultured neurons (Tang et al., 2003). The balance of the excitatory and inhibitory neurotransmission within neuronal networks largely controls SCO patterns and require membrane electrical activity (Dravid and Murray, 2004, Cao et al., 2012a), although the relationship between these two fundamental processes that are not fully understood and likely differ among specific brain neural networks and developmental stage. SCO activity is critical not only to activity dependent growth of neurons (Kerschensteiner et

al., 2009) but also the refinement and strengthening of long-range synaptic architecture (Saneyoshi et al., 2010, Basu and Siegelbaum, 2015, Lee et al., 2016).

In the present report, we show the temporal differences of SCO patterns in two types of developing hippocampal neuronal networks in culture; enriched hippocampal neurons (HN) with few (<5%) glia, and hippocampal neuron/glia co-cultures (HNA). As HN developed more complex morphology *in vitro*, the temporal pattern and amplitude of the SCOs they generate also become more complex. Positive regulation of SCO activity relies on excitatory glutamatergic neurotransmission driven by both ionotropic as well as metabotropic glutamate receptors (mGluR) (Dravid and Murray, 2004, Koga et al., 2010, Hongo et al., 2015). $GABA_A$ receptor activity was also associated with changing SCOs patterns. Both positive and negative modulation of $GABA_A$ receptor function affects electrical firing patterns as well as the SCO behavior (Cao et al., 2012a, Cao et al., 2012b). Therefore, the balance of excitatory and inhibitory neurotransmission intrinsic within the HN and HNG networks shapes SCOs patterns as they develop. We demonstrated that the expression levels of vGAT were unchanged within the developmental time frame studied, whereas vGLUT1 expression levels significantly increased with DIV and was associated with increasing SCO activity in HN cultures. We also demonstrate that the level of expression of synaptic $\gamma 2$ and extrasynaptic $\alpha 5$ $GABA_A$ receptor subunits are developmentally regulated in HN cultures. Although *in vivo* $GABA_A$ receptor expression during early postnatal development transits from excitatory to inhibitory (Galanopoulou, 2008), in our murine HN and HNG culture models, the $GABA_A$ receptor blocker TETS elicits similar patterns of enhanced neuroexcitability as early as 6 DIV, indicating a consistent inhibitory role of $GABA_A$ receptors. It should be mentioned that the mechanisms contributing to SCO generation are complex and many mechanisms participate in defining SCOs patterns. For example, modulation of K^+ channels (Cao et al., 2014), kainate receptors (Saneyoshi et al., 2010) and intracellular Ca^{2+} release channels such as ryanodine receptors (Wayman et al., 2012) as well as IP_3 receptors (Dravid and Murray, 2004). The NMDA receptor also contributes to the shaping of SCOs and NMDA receptor subunits undergo expression shifts that could also contribute to regulation of SCO patterns during HN and HNG network development (Cserep et al., 2012). However, the relationship between NMDA receptor subtype transition and SCO pattern during development needs further exploration.

Astrocytes have a major influence on neuronal network development both structurally and functionally (Lopez-Hidalgo and Schummers, 2014, Chung et al., 2015). It should be mentioned that the SCOs measured in current study in the HNG cultures originated from neurons since the Ca^{2+} oscillations in astrocytes are asynchronous and have much longer durations than those measured from the neuronal networks (Cao et al., 2013). Our data clearly demonstrate that astrocytes influence the onset and pattern of SCOs during HNG culture development. The molecular mechanism for how astrocytes influence the formation of neuronal network activity needs further investigation. However, a number of factors likely contribute to the different patterns observed with HN and HNG cultures. For example, astrocytes have been demonstrated to alter synapse formation (Chung et al., 2015). In addition, the high percentage of glia present in the HNG cultures can influence synchronous electrical firing by altering Glu signaling through the activity of astrocytic glutamate transporters, which uptake Glu (Swanson et al., 1997, Perego et al., 2000), as well as

influencing GABAergic synapse signaling and density (Elmariah et al., 2005, Hughes et al., 2010).

TETS produced distinct changes in SCO dynamics in HN *vs.* HNG cultures that were dependent on their *in vitro* age. Although the potencies for TETS suppressing SCO frequency and increasing the SCO amplitude (Phase II response) on the 6, 9, 14 DIV HN cultures were comparable, the maximal amplitude increase produced by TETS increased as HN cultures matured. TETS also produced an acute increase on the intracellular Ca^{2+} concentration (Phase I response) in HN cultures at 14 DIV, which was not observed in HN cultures ≤9 DIV. These data overall suggest that older HN cultures are more sensitive to TETS. We also demonstrated that α5 subunits expression levels continued to rise as HN cultures matured. It should be mentioned that the acute "Phase I" rise in intracellular Ca^{2+} triggered by TETS relies on glutamate neurotransmission and activation of the NMDA receptors (Cao et al., 2012a). Although the current study did not delineate why less mature (6 and 9 DIV) hippocampal neurons lack a Phase I response to TETS, our results suggest that suppression of $GABA_A$ receptor signaling was insufficient to tip the excitatory/inhibitory balance of less developed HN cultures to elicit a measurable glutamatergic Phase I response.

Challenging 6 DIV HNG cultures with TETS increased SCO amplitude as well as decreased the SCO frequency although the maximal reduction on SCOs amplitude is much smaller than that observed in 6 DIV HN cultures. However, 9 DIV HNG cultures appeared to be insensitive to the TETS exposure. These observations are consistent with previous study that reported PTX as high as 100 μM was without effect on both SCOs frequency and amplitude in a relatively low density 12 DIV HNG culture (Bacci et al., 1999). Therefore, the responsiveness of HNG cultures to TETS appears to be more highly dependent on developmental stage compared to HN cultures. The detailed mechanism underlying these divergent responses to TETS likely involves the role of astrocytes in mitigating over-excitation of glutamatergic neurotransmission, but needs further investigation. TETS triggered Ca^{2+} responses that were normalized by NMDA receptor antagonist (Cao et al., 2012a). NMDA receptor antagonist also suppressed PTX-induced Ca^{2+} responses as well as the frequency and duration of the epileptiform discharges in the hippocampal slice preparation (Kohr and Heinemann, 1989). Blockade of NMDA receptors also normalized TETS, PTX or bicuculline-induced seizure (Czlonkowska et al., 2000, Shakarjian et al., 2015). NMDA receptor activation following $GABA_A$ receptor blockade has also been demonstrated to enhance synaptic glutamatergic neurotransmission (Hardingham et al., 2002). Astrocytes play a pivotal role on the Glu reuptake through Glu transporters, mainly GLAST and GLT1 (Rothstein et al., 1996). Here we demonstrated that astrocytes increased in HNG with time in culture. Therefore, it is possible that astrocytes rapidly buffer excess glutamate subsequent to TETS exposure, a biologically plausible mechanism given that TETS-modified SCO patterns can largely be normalized in the presence of NMDA receptor antagonist (Cao et al., 2012a, Shakarjian et al., 2015). In addition, enhanced GABAergic activity and GABA synapse density may also contribute to the relative insensitivity of TETS in HNG cultures (Elmariah et al., 2005, Hughes et al., 2010).

SCOs are dependent on membrane electrical activity since tetrodotoxin completely abolished SCOs in HN cultures (Supplemental Fig. 1), consistent with the previous reports (Dravid and Murray, 2004). In addition, both TETS and PTX can induce burst like electric activity in HN cultures (Cao et al., 2012b) suggesting that SCO in cultured neurons are associated with neuroexcitability; a fundamental cause for seizure induction. Additionally, synchronized electric firing of a population of neurons also contributes to seizure induction. Our observation that TETS-triggered increase in SCO amplitude (Phase II response) are closely associated with and dependent on highly synchronized electric spike activity implies their relevance as a model of seizure-like activity observed *in vivo*. NMDA receptors activation has been well documented to contribute to the neuroexcitatoxicity. In 14 DIV HN, we also observed a sustained $[Ca^{2+}]_i$ overloading which can be abolished by the NMDA receptor antagonist, MK-801 (Cao et al., 2012a). The results of recent studies indicate that application of MK-801 or ketamine more effectively prevents TETS-induced lethality compared to the prevention on TETS-induced tonic-clonic seizures suggesting the Phase I response contributes to the delayed pathology of TETS which has been observed in experimental and clinical studies (Cheng et al., 2002, Deng et al., 2012, Zolkowska et al., 2012, Vito et al., 2014, Bruun et al., 2015). In our *in vitro* study, HN/HNG responded to TETS differentially with distinct efficacy on the amplification of SCO amplitude. Whether the distinct efficacy of TETS on SCO amplitude is associated with the severity of TETS-induced seizure needs further examination since no literature data available to directly compare the TETS intoxication sensitivity/severity *in vivo*.

The LD_{50} values for TETS with intraperitoneal or oral administration recently determined were 0.28 and 0.22 mg/kg in rat, respectively (Zolkowska et al., 2012). When administered orally, TETS is 40 times more potent than PTX, however when administered intraventricularly to mice they have similar potencies to induce seizure and lethality (Zolkowska et al., 2012). Since we demonstrated here that PTX and TETS produced similar patterns of SCO abnormalities in HN and with similar potencies, it is likely that the discrepancy between the potencies of TETS and PTX to induce seizure and lethality when administered orally or intravenously stems from differences in their *in vivo* pharmacokinetics.

In summary, we demonstrated that both HN and HNG cultures displayed developmental changes on the SCOs patterns using rapid throughput Ca^{2+} recording. The developmental SCOs patterns in HN cultures appear to be associated with the balance of excitatory/inhibitory inputs. In addition, we demonstrated that differential responses to TETS in HN and HNG cultures depend on developmental stages and the presence of glia in the culture.

Supplementary Material

Refer to Web version on PubMed Central for supplementary material.

Acknowledgments

This study was supported by NINDS (grant number 1U54 NS079202), the Chinese Natural Science Foundation (grant number 81473539), the Jiangsu Provincial Natural Science Foundation (grant number BK20141357).

Abbreviations

ARA-C	cytosine β-D-arabinofuranoside
$[Ca^{2+}]_i$	intracellular Ca^{2+} concentration
AUC	area under curve
CI	confidence intervals
DIV	days in vitro
FLIPR	Fluorescent Imaging Plate Reader
GFAP	glial fibrillary acidic protein
GABA	γ-aminobutyric acid
HN	hippocampal neuronal cultures
HNG	hippocampal neuron/glia co-cultures
MAP-2B	microtubule-associated protein-2B
PTX	picrotoxin
SCO	spontaneous Ca^{2+} oscillations
TETS	tetramethylenedisulfotetramine
vGAT	vesicular GABA transporter
vGLUT1	vesicular glutamate transporter 1

References

Bacci A, Verderio C, Pravettoni E, Matteoli M. Synaptic and intrinsic mechanisms shape synchronous oscillations in hippocampal neurons in culture. Eur J Neurosci. 1999; 11:389–397. [PubMed: 10051739]

Balschun D, Moechars D, Callaerts-Vegh Z, Vermaercke B, Van Acker N, Andries L, D'Hooge R. Vesicular glutamate transporter VGLUT1 has a role in hippocampal long-term potentiation and spatial reversal learning. Cereb Cortex. 2010; 20:684–693. [PubMed: 19574394]

Bando Y, Irie K, Shimomura T, Umeshima H, Kushida Y, Kengaku M, Fujiyoshi Y, Hirano T, Tagawa Y. Control of Spontaneous Ca2+ Transients Is Critical for Neuronal Maturation in the Developing Neocortex. Cereb Cortex. 2016; 26:106–117. [PubMed: 25112282]

Barrueto F Jr, Furdyna PM, Hoffman RS, Hoffman RJ, Nelson LS. Status epilepticus from an illegally imported Chinese rodenticide: "tetramine". J Toxicol Clin Toxicol. 2003; 41:991–994. [PubMed: 14705847]

Basu J, Siegelbaum SA. The Corticohippocampal Circuit, Synaptic Plasticity, and Memory. Cold Spring Harb Perspect Biol. 2015; 7

Bateup HS, Johnson CA, Denefrio CL, Saulnier JL, Kornacker K, Sabatini BL. Excitatory/inhibitory synaptic imbalance leads to hippocampal hyperexcitability in mouse models of tuberous sclerosis. Neuron. 2013; 78:510–522. [PubMed: 23664616]

Bellocchio EE, Reimer RJ, Fremeau RT Jr, Edwards RH. Uptake of glutamate into synaptic vesicles by an inorganic phosphate transporter. Science. 2000; 289:957–960. [PubMed: 10938000]

Bruun DA, Cao Z, Inceoglu B, Vito ST, Austin AT, Hulsizer S, Hammock BD, Tancredi DJ, Rogawski MA, Pessah IN, Lein PJ. Combined treatment with diazepam and allopregnanolone reverses tetramethylenedisulfotetramine (TETS)-induced calcium dysregulation in cultured neurons and protects TETS-intoxicated mice against lethal seizures. Neuropharmacology. 2015; 95:332–342. [PubMed: 25882826]

Cao Z, Cui Y, Busse E, Mehrotra S, Rainier JD, Murray TF. Gambierol inhibition of voltage-gated potassium channels augments spontaneous Ca2+ oscillations in cerebrocortical neurons. J Pharmacol Exp Ther. 2014; 350:615–623. [PubMed: 24957609]

Cao Z, Hammock BD, McCoy M, Rogawski MA, Lein PJ, Pessah IN. Tetramethylenedisulfotetramine alters Ca(2)(+) dynamics in cultured hippocampal neurons: mitigation by NMDA receptor blockade and GABA(A) receptor-positive modulation. Toxicol Sci. 2012a; 130:362–372. [PubMed: 22889812]

Cao Z, Hulsizer S, Cui Y, Pretto DL, Kim KH, Hagerman PJ, Tassone F, Pessah IN. Enhanced asynchronous Ca(2+) oscillations associated with impaired glutamate transport in cortical astrocytes expressing Fmr1 gene premutation expansion. J Biol Chem. 2013; 288:13831–13841. [PubMed: 23553633]

Cao Z, Hulsizer S, Tassone F, Tang HT, Hagerman RJ, Rogawski MA, Hagerman PJ, Pessah IN. Clustered burst firing in FMR1 premutation hippocampal neurons: amelioration with allopregnanolone. Hum Mol Genet. 2012b; 21:2923–2935. [PubMed: 22466801]

Cao Z, Zou X, Cui Y, Hulsizer S, Lein PJ, Wulff H, Pessah IN. Rapid throughput analysis demonstrates that chemicals with distinct seizurogenic mechanisms differentially alter Ca2+ dynamics in networks formed by hippocampal neurons in culture. Mol Pharmacol. 2015; 87:595–605. [PubMed: 25583085]

Chen Y, Stevens B, Chang J, Milbrandt J, Barres BA, Hell JW. NS21: re-defined and modified supplement B27 for neuronal cultures. J Neurosci Methods. 2008; 171:239–247. [PubMed: 18471889]

Cheng YB, Liu NG, Zhang JH. Apoptosis in mouse after tetramine poisoning. Fa Yi Xue Za Zhi. 2002; 18:137–139. 143. [PubMed: 12608289]

Chung WS, Allen NJ, Eroglu C. Astrocytes Control Synapse Formation, Function, and Elimination. Cold Spring Harb Perspect Biol. 2015; 7:a020370. [PubMed: 25663667]

Clause A, Kim G, Sonntag M, Weisz CJ, Vetter DE, Rubsamen R, Kandler K. The precise temporal pattern of prehearing spontaneous activity is necessary for tonotopic map refinement. Neuron. 2014; 82:822–835. [PubMed: 24853941]

Cserep C, Szabadits E, Szonyi A, Watanabe M, Freund TF, Nyiri G. NMDA receptors in GABAergic synapses during postnatal development. PLoS One. 2012; 7:e37753. [PubMed: 22662211]

Czlonkowska AI, Krzascik P, Sienkiewicz-Jarosz H, Siemiatkowski M, Szyndler J, Bidzinski A, Plaznik A. The effects of neurosteroids on picrotoxin-, bicuculline- and NMDA-induced seizures, and a hypnotic effect of ethanol. Pharmacol Biochem Behav. 2000; 67:345–353. [PubMed: 11124400]

Deng X, Li G, Mei R, Sun S. Long term effects of tetramine poisoning: an observational study. Clin Toxicol (Phila). 2012; 50:172–175. [PubMed: 22315994]

Dravid SM, Murray TF. Spontaneous synchronized calcium oscillations in neocortical neurons in the presence of physiological [Mg(2+)]: involvement of AMPA/kainate and metabotropic glutamate receptors. Brain Res. 2004; 1006:8–17. [PubMed: 15047019]

Elmariah SB, Oh EJ, Hughes EG, Balice-Gordon RJ. Astrocytes regulate inhibitory synapse formation via Trk-mediated modulation of postsynaptic GABAA receptors. J Neurosci. 2005; 25:3638–3650. [PubMed: 15814795]

Flannery BM, Silverman JL, Bruun DA, Puhger KR, McCoy MR, Hammock BD, Crawley JN, Lein PJ. Behavioral assessment of NIH Swiss mice acutely intoxicated with tetramethylenedisulfotetramine. Neurotoxicol Teratol. 2015; 47:36–45. [PubMed: 25446016]

Galanopoulou AS. GABA(A) receptors in normal development and seizures: friends or foes? Curr Neuropharmacol. 2008; 6:1–20. [PubMed: 19305785]

George J, Dravid SM, Prakash A, Xie J, Peterson J, Jabba SV, Baden DG, Murray TF. Sodium channel activation augments NMDA receptor function and promotes neurite outgrowth in immature cerebrocortical neurons. J Neurosci. 2009; 29:3288–3301. [PubMed: 19279266]

Hardingham GE, Fukunaga Y, Bading H. Extrasynaptic NMDARs oppose synaptic NMDARs by triggering CREB shut-off and cell death pathways. Nat Neurosci. 2002; 5:405–414. [PubMed: 11953750]

Hongo Y, Takasu K, Ikegaya Y, Hasegawa M, Sakaguchi G, Ogawa K. Heterogeneous effects of antiepileptic drugs in an in vitro epilepsy model–a functional multineuron calcium imaging study. Eur J Neurosci. 2015; 42:1818–1829. [PubMed: 25967117]

Hughes EG, Elmariah SB, Balice-Gordon RJ. Astrocyte secreted proteins selectively increase hippocampal GABAergic axon length, branching, and synaptogenesis. Mol Cell Neurosci. 2010; 43:136–145. [PubMed: 19850128]

Jabba SV, Prakash A, Dravid SM, Gerwick WH, Murray TF. Antillatoxin, a novel lipopeptide, enhances neurite outgrowth in immature cerebrocortical neurons through activation of voltage-gated sodium channels. J Pharmacol Exp Ther. 2010; 332:698–709. [PubMed: 20026674]

Jang MJ, Nam Y. NeuroCa: integrated framework for systematic analysis of spatiotemporal neuronal activity patterns from large-scale optical recording data. Neurophotonics. 2015; 2:035003. [PubMed: 26229973]

Kerschensteiner D, Morgan JL, Parker ED, Lewis RM, Wong ROL. Neurotransmission selectively regulates synapse formation in parallel circuits in vivo. Nature. 2009; 460:1016–U1103. [PubMed: 19693082]

Koga K, Iwahori Y, Ozaki S, Ohta H. Regulation of spontaneous Ca(2+) spikes by metabotropic glutamate receptors in primary cultures of rat cortical neurons. Journal of Neuroscience Research. 2010; 88:2252–2262. [PubMed: 20209633]

Kohr G, Heinemann U. Effects of NMDA antagonists on picrotoxin-, low Mg2+- and low Ca2+-induced epileptogenesis and on evoked changes in extracellular Na+ and Ca2+ concentrations in rat hippocampal slices. Epilepsy Res. 1989; 4:187–200. [PubMed: 2575519]

Lee KF, Soares C, Thivierge JP, Beique JC. Correlated Synaptic Inputs Drive Dendritic Calcium Amplification and Cooperative Plasticity during Clustered Synapse Development. Neuron. 2016; 89:784–799. [PubMed: 26853305]

Lopez-Hidalgo M, Schummers J. Cortical maps: a role for astrocytes? Curr Opin Neurobiol. 2014; 24:176–189. [PubMed: 24419141]

McIntire SL, Reimer RJ, Schuske K, Edwards RH, Jorgensen EM. Identification and characterization of the vesicular GABA transporter. Nature. 1997; 389:870–876. [PubMed: 9349821]

Patel TP, Man K, Firestein BL, Meaney DF. Automated quantification of neuronal networks and single-cell calcium dynamics using calcium imaging. J Neurosci Methods. 2015; 243:26–38. [PubMed: 25629800]

Perego C, Vanoni C, Bossi M, Massari S, Basudev H, Longhi R, Pietrini G. The GLT-1 and GLAST glutamate transporters are expressed on morphologically distinct astrocytes and regulated by neuronal activity in primary hippocampal cocultures. J Neurochem. 2000; 75:1076–1084. [PubMed: 10936189]

Puranam RS, He XP, Yao L, Le T, Jang W, Rehder CW, Lewis DV, McNamara JO. Disruption of Fgf13 causes synaptic excitatory-inhibitory imbalance and genetic epilepsy and febrile seizures plus. J Neurosci. 2015; 35:8866–8881. [PubMed: 26063919]

Ratra GS, Kamita SG, Casida JE. Role of human GABA(A) receptor beta3 subunit in insecticide toxicity. Toxicol Appl Pharmacol. 2001; 172:233–240. [PubMed: 11312652]

Rothstein JD, Dykes-Hoberg M, Pardo CA, Bristol LA, Jin L, Kuncl RW, Kanai Y, Hediger MA, Wang Y, Schielke JP, Welty DF. Knockout of glutamate transporters reveals a major role for astroglial transport in excitotoxicity and clearance of glutamate. Neuron. 1996; 16:675–686. [PubMed: 8785064]

Saneyoshi T, Fortin DA, Soderling TR. Regulation of spine and synapse formation by activity-dependent intracellular signaling pathways. Curr Opin Neurobiol. 2010; 20:108–115. [PubMed: 19896363]

Shakarjian MP, Ali MS, Veliskova J, Stanton PK, Heck DE, Velisek L. Combined diazepam and MK-801 therapy provides synergistic protection from tetramethylenedisulfotetramine-induced tonic-clonic seizures and lethality in mice. Neurotoxicology. 2015; 48:100–108. [PubMed: 25783504]

Spitzer NC. Electrical activity in early neuronal development. Nature. 2006; 444:707–712. [PubMed: 17151658]

Squires RF, Casida JE, Richardson M, Saederup E. [35S]t-butylbicyclophosphorothionate binds with high affinity to brain-specific sites coupled to gamma-aminobutyric acid-A and ion recognition sites. Mol Pharmacol. 1983; 23:326–336. [PubMed: 6300642]

Swanson RA, Liu J, Miller JW, Rothstein JD, Farrell K, Stein BA, Longuemare MC. Neuronal regulation of glutamate transporter subtype expression in astrocytes. J Neurosci. 1997; 17:932–940. [PubMed: 8994048]

Tang F, Dent EW, Kalil K. Spontaneous calcium transients in developing cortical neurons regulate axon outgrowth. J Neurosci. 2003; 23:927–936. [PubMed: 12574421]

Vito ST, Austin AT, Banks CN, Inceoglu B, Bruun DA, Zolkowska D, Tancredi DJ, Rogawski MA, Hammock BD, Lein PJ. Post-exposure administration of diazepam combined with soluble epoxide hydrolase inhibition stops seizures and modulates neuroinflammation in a murine model of acute TETS intoxication. Toxicol Appl Pharmacol. 2014; 281:185–194. [PubMed: 25448683]

Wayman GA, Yang D, Bose DD, Lesiak A, Ledoux V, Bruun D, Pessah IN, Lein PJ. PCB-95 promotes dendritic growth via ryanodine receptor-dependent mechanisms. Environ Health Perspect. 2012; 120:997–1002. [PubMed: 22534141]

Whitlow KS, Belson M, Barrueto F, Nelson L, Henderson AK. Tetramethylenedisulfotetramine: old agent and new terror. Ann Emerg Med. 2005; 45:609–613. [PubMed: 15940093]

Zhao C, Hwang SH, Buchholz BA, Carpenter TS, Lightstone FC, Yang J, Hammock BD, Casida JE. GABAA receptor target of tetramethylenedisulfotetramine. Proc Natl Acad Sci U S A. 2014; 111:8607–8612. [PubMed: 24912155]

Zolkowska D, Banks CN, Dhir A, Inceoglu B, Sanborn JR, McCoy MR, Bruun DA, Hammock BD, Lein PJ, Rogawski MA. Characterization of seizures induced by acute and repeated exposure to tetramethylenedisulfotetramine. J Pharmacol Exp Ther. 2012; 341:435–446. [PubMed: 22328574]

Highlights

- Hippocampal neuronal cultures (HN) and neuron/glia co-cultures (HNG) form networks
- HN and HNA networks show spontaneous *synchronous Ca^{2}+ oscillations* (SCO)
- HN and HNG display distinct SCO patterns during development
- The developmental patterns of SCO in HN and HNG may associated with excitatory/inhibitory balance
- HN and HNG exhibit differential responses to TETS that are dependent on developmental stage.

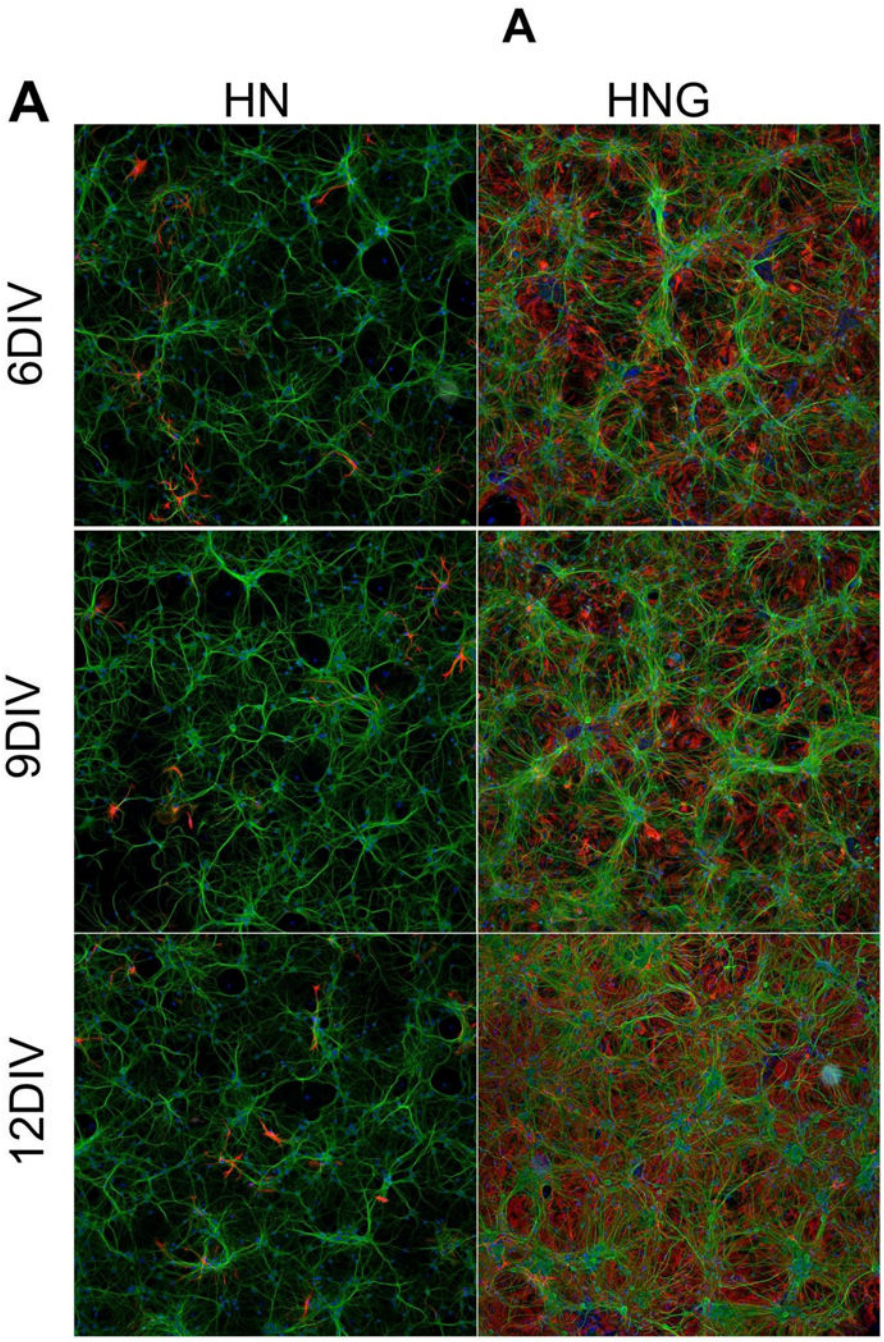

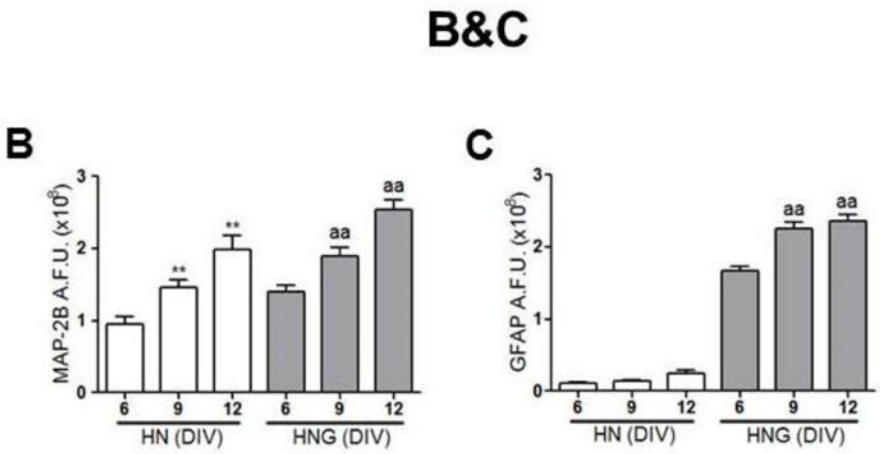

Figure 1. MAP-2B and GFAP immunostaining in 6, 9, 12 DIV HN and HNG cultures

(A) Representative MAP-2B and GFAP staining pictures in 6, 9, 12 DIV hippocampal neurons in the presence (HN, left panel) and absence (HNG, right panel) of ARA-C post exposure; (B) Quantification of the MAP-2B fluorescence intensity in 6, 9, 12 DIV HN and HNG cultures; (C) Quantification of the GFAP fluorescence intensity in 6, 9, 12 DIV HN and HNG cultures. Each data point represents Mean±SEM from two independent experiments performed in triplicates. **, $p<0.01$, *vs.* 6 DIV HN; ^{aa}, $p<0.01$, *vs.* 6 DIV HNG. Green, MAP-2B; Red, GFAP; Blue; Hoechst-33342.

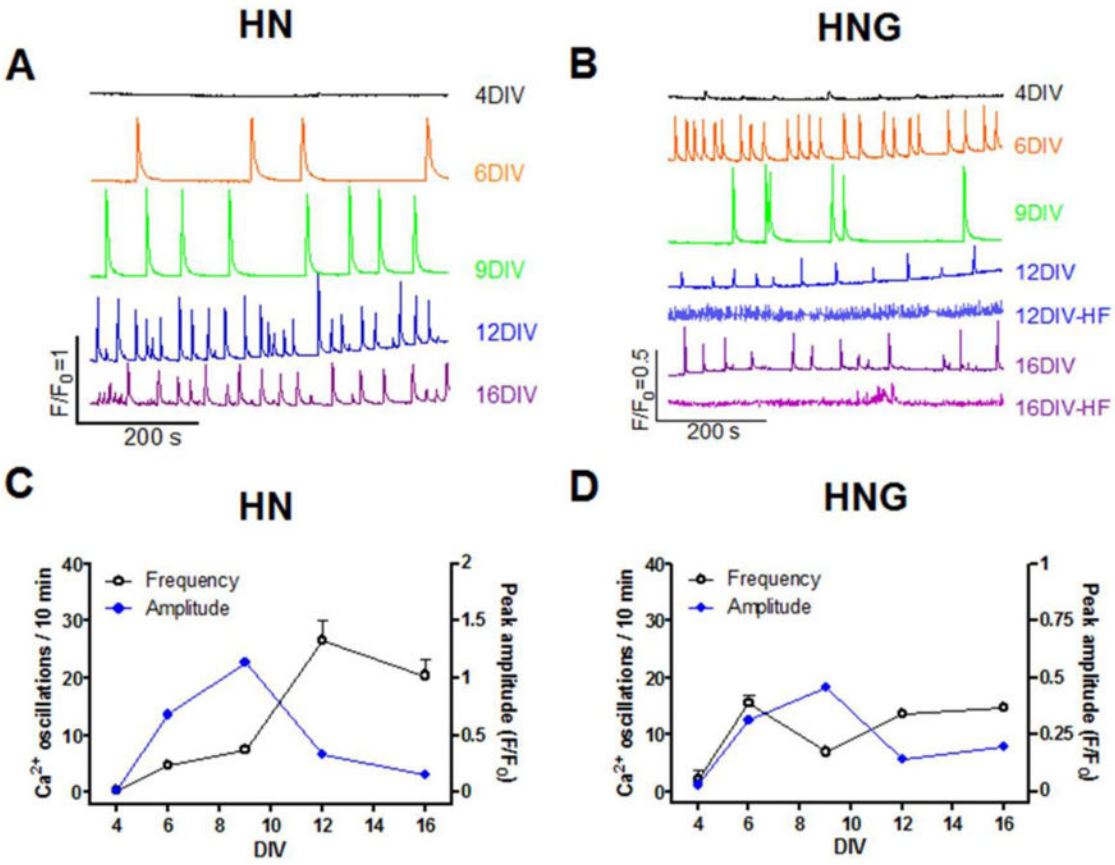

Figure 2. SCOs patterns in HN and HNG cultures at different ages

Representative traces of SCOs in HN (A) and HNG (B) at different ages; Quantification of SCO frequency and amplitude in different ages of HN (C) and HNG (D). Each data point of frequency represents Mean±SEM from at least three independent cultures performed in five replicates and each data point of amplitude represents Mean±SEM of all the SCO events from three independent cultures performed in five replicates. It should be noted that although five batches of HNG cultures displayed consistent developmental patterns of SCOs until 9 DIV, 2 out of 5 cultures displayed a very high frequency (HF) low amplitude events commencing greater than 12 DIV. Since the amplitude of SCOs from these traces was smaller than 0.1 units ($\Delta F/F_0$), we didn't quantify the frequency and amplitude of these high frequent SCOs.

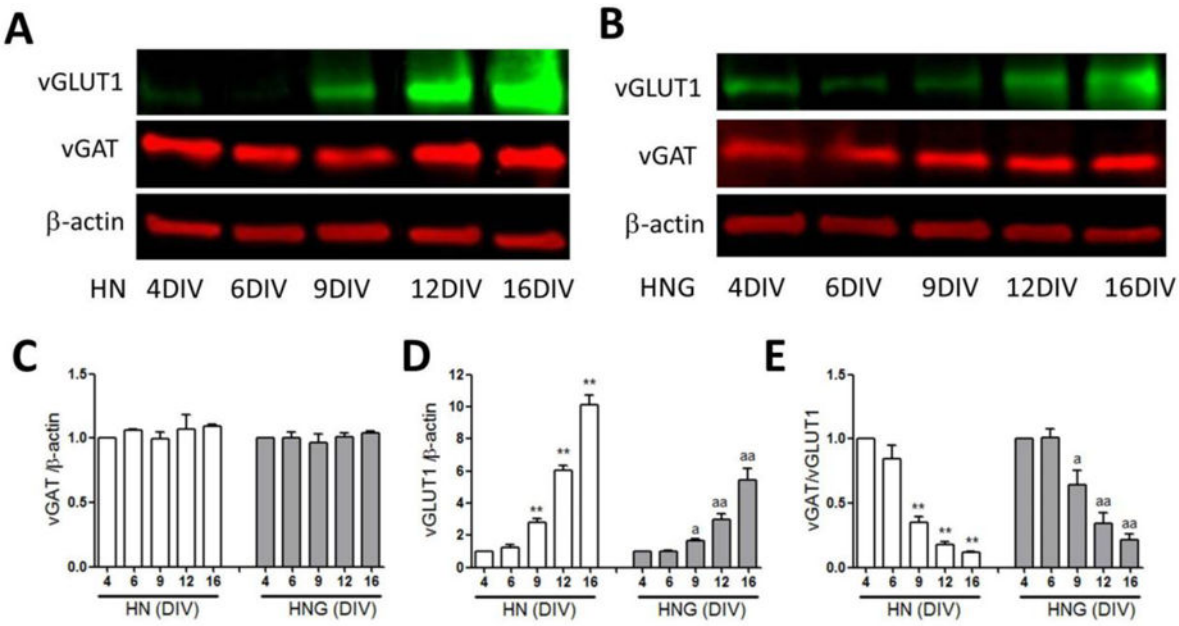

Figure 3. Expression levels of vGAT and vGLUT1 in 4, 6, 9, 12 and 16 DIV cultures

Representative western blots for vGAT and vGLUT1 expressions in 4, 6, 9, 12 and 16 DIV HN (A) and HNG (B) cultures; Quantification of the vGAT (C) and vGLUT1 (D) expression levels in 4, 6, 9, 12 and 16 DIV HN and HNG cultures; (E) The ratio of vGAT over vGLUT1 expression in 4, 6, 9, 12 and 16 DIV cultures. Each data point represents the Mean±SEM (n=4) pooled from two independent cultures. *, $p<0.05$, **, $p<0.01$ *vs.* 4 DIV HN cultures; [a], $p<0.05$, [aa], $p<0.01$ *vs.* 4 DIV HNG cultures.

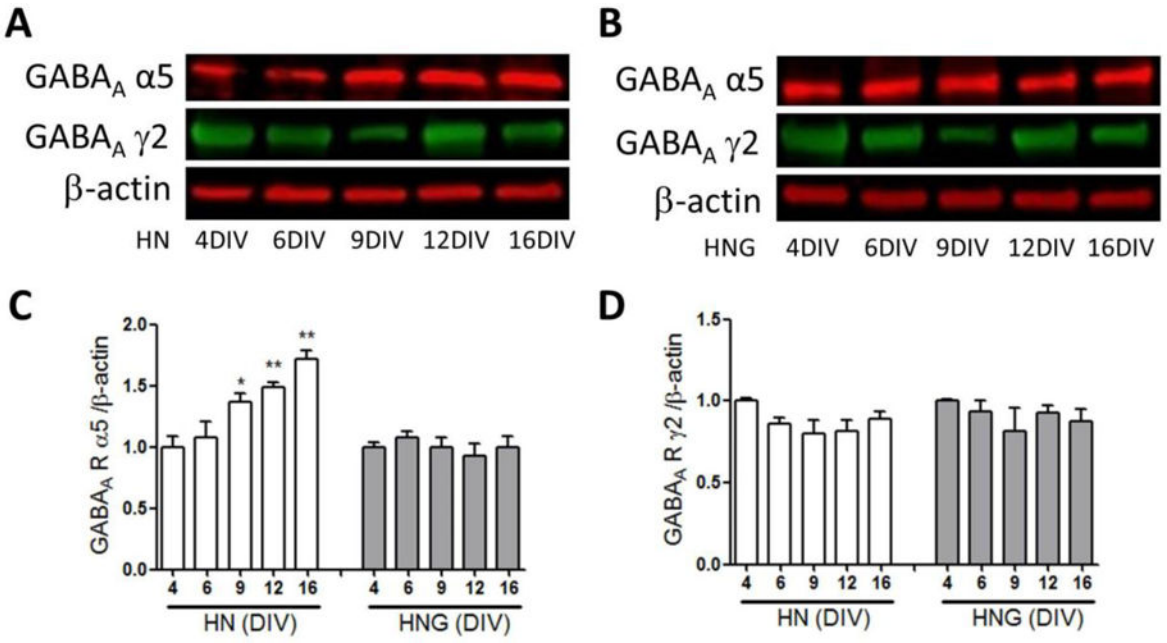

Figure 4. Expression levels of GABA$_A$ receptor γ2 and α5 subunits in 4, 6, 9, 12 and 16 DIV cultures

Representative western blot for GABA$_A$ receptors γ_2 and α_5 subunits expressions in 4, 6, 9, 12 and 16 DIV HN (A) and HNG (B) cultures; Quantification of the GABA$_A$ receptor α5 (C) and GABA$_A$ receptor γ2 (D) subunits expression levels in 4, 6, 9, 12 and 16 DIV cultures. Each data point represents the Mean±SEM (n=4) pooled from two independent cultures. *, $p<0.05$, **, $p<0.01$, *vs.* 4 DIV HN culture.

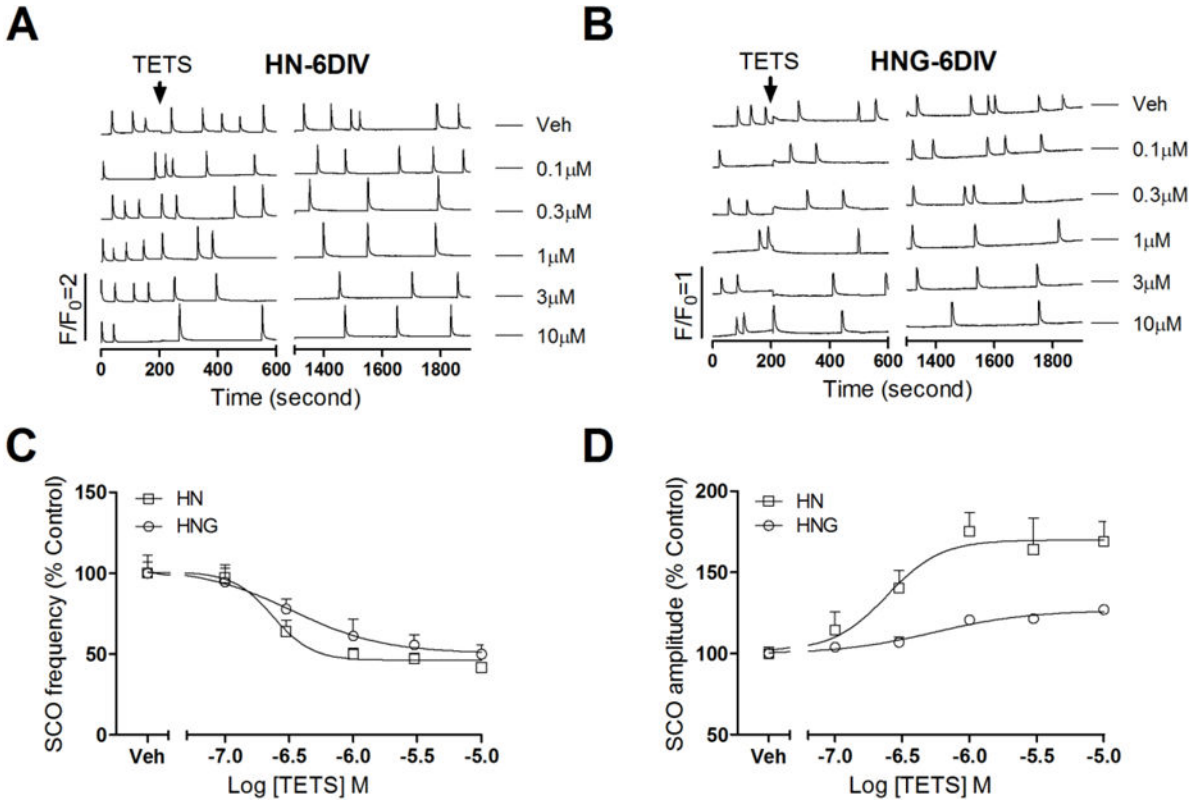

Figure 5. TETS response on the SCOs in HNG and HN cultures at 6 DIV

Representative traces of TETS response on the SCOs as a function of time in 6 DIV HN (A) and HNG (B) cultures. The effects of TETS were analyzed during an epoch of 10 min after addition of TETS for 20 min (Phase II response); (C) TETS caused a concentration-dependent decrease in SCO frequency in both HN and HNG cultures with IC_{50} values of 0.22 μM (0.12–0.43 μM, 95%CI) and 0.33 μM (0.08–1.45 μM, 95%CI), respectively; (D) TETS caused a concentration-dependent increase in the mean amplitude of SCOs in both HN and HNG cultures with EC_{50} values of 0.24 μM (0.10–0.60 μM, 95%CI) and 0.56 μM (0.27–1.36 μM, 95%CI), respectively. This experiment was repeated in two independent cultures, each with four replicates.

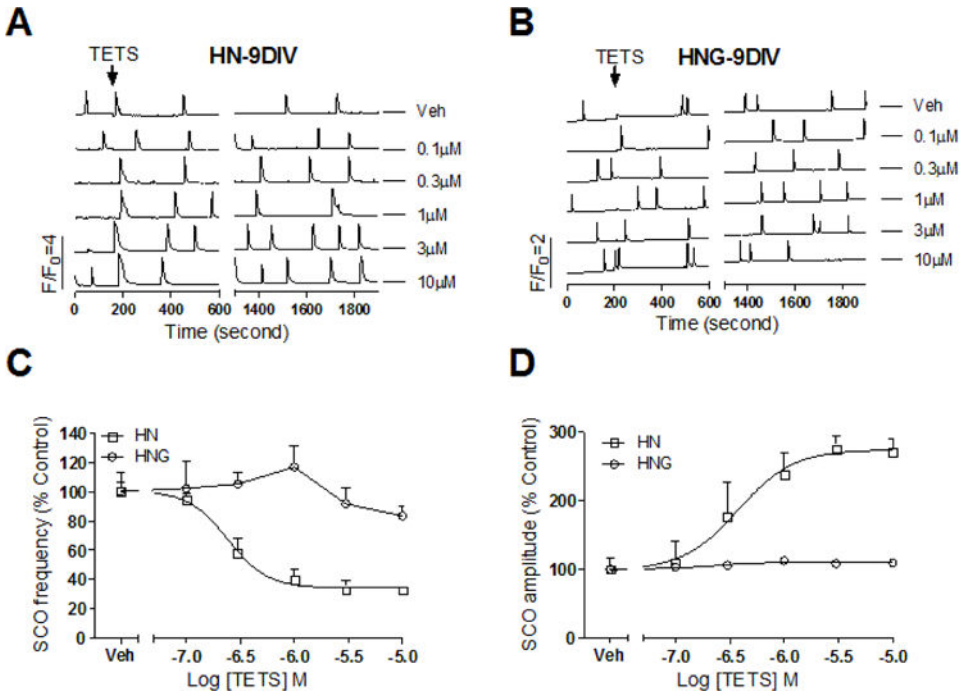

Figure 6. TETS response on SCO in HN and HNG cultures at 9 DIV

Representative traces of TETS response on the SCOs as a function of time in HN (A) and HNG (B) cultures at 9 DIV. The effects of TETS were analyzed during an epoch of 10 min after addition of TETS for 20 min (Phase II response); (C) TETS caused a concentration-dependent decrease in SCO frequency with an IC_{50} value of 0.24 μM (0.16–0.38 μM, 95%CI) with 65.8% maximal inhibition. TETS had no response on SCO frequency in HNG cultures at 9 DIV; (D) TETS produced a concentration-dependent increase in the mean SCO amplitude with an EC_{50} value of 0.37 μM (0.15–0.96 μM, 95%CI) with maximal increase of 174% of control. TETS had no response in 9 DIV HNG cultures. This experiment was repeated in two independent cultures, each with four replicates.

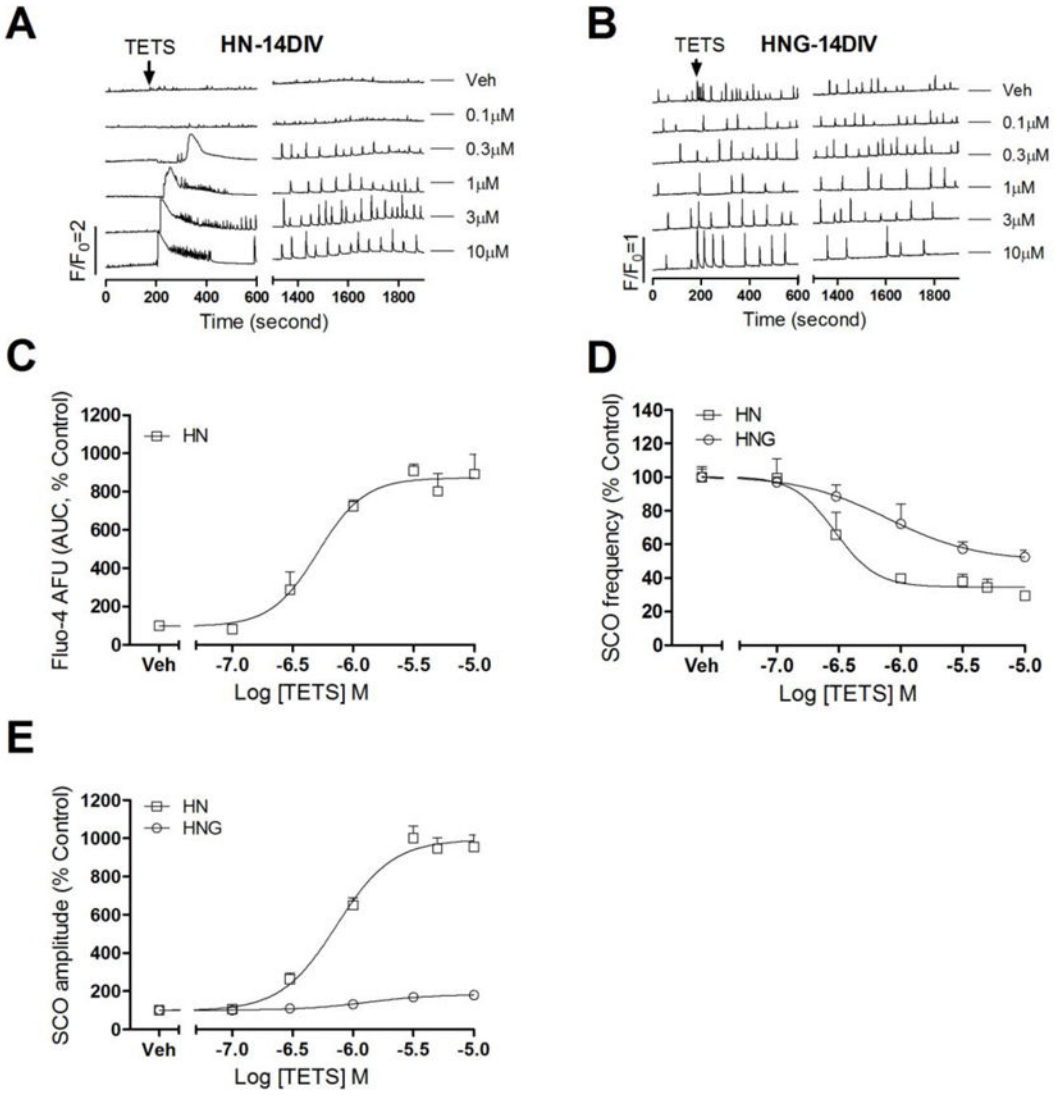

Figure 7. TETS response on SCO in HNG and HN cultures at 14 DIV

Representative traces of TETS response on SCOs as a function of time in HN (A) and HNG (B) cultures at 14 DIV. In addition to delayed increased SCO amplitude and decreased SCO frequency (Phase II response), TETS produced an immediate intracellular Ca^{2+} rising (Phase I response) in 14 DIV HN; (C) Concentration-response relationships for TETS-induced intracellular Ca^{2+} rising calculated as Fluo-4 fluorescence area under the curve (AUC); The AUC was calculated in a period of 10 min after TETS addition; (D) Concentration-response relationships for TETS decreased SCO frequency in 14 DIV HNG and HN cultures; (E) Concentration-response relationships for TETS increased SCO amplitude in 14 DIV HNG and HN cultures. This experiment was repeated in three independent cultures, each with four replicates.

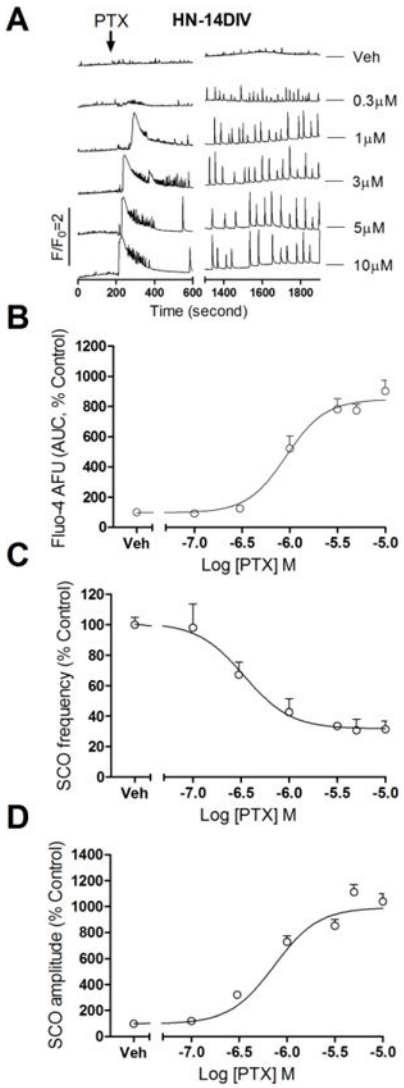

Figure 8. Pictotoxin response on SCO in HN cultures at 14 DIV

(A) Representative traces of picrotoxin (PTX) response on SCO as a function of time in HN cultures at 14 DIV. Similar to the TETS response in 14 DIV HN, picrotoxin produced an immediate intracellular Ca^{2+} rising (Phase I response) and a delayed SCO frequency decrease accompanied with SCO amplitude increase (Phase II response); (B) Concentration-response relationships for picrotoxin-induced intracellular Ca^{2+} rising calculated as Fluo-4 fluorescence area under the curve (AUC); (C) Concentration-response relationships for picrotoxin-induced SCO frequency decrease; (D) Concentration-response relationships for picrotoxin-induced SCO amplitude increase. This experiment was repeated in two independent cultures, each with four replicates.

Table 1

Summary of the potency and maximum response of TETS Phase I and Phase II responses on SCO in HN or HNG cultures 6, 9, 14 DIVs.

		Phase I (AUC)		Phase II			
				Frequency		Amplitude	
		EC_{50}(μM) (95%CI)	Max. incre. (95%CI)	IC_{50}(μM) (95%CI)	Max. inhib. (95%CI)	EC_{50}(μM) (95%CI)	Max. incre. (95%CI)
6 DIV	HN	NR	NR	0.22 (0.12–0.43)	51.7% (43.5%–59.8%)	0.24 (0.10–0.60)	70.5% (47.0%–93.9%)
	HNG	NR	NR	0.33 (0.08–1.45)	49.6% (30.0%–69.3%)	0.56 (0.27–1.36)	26.6% (18.0%–35.2%)
9 DIV	HN	NR	NR	0.24 (0.16–0.38)	65.8% (56.5%–75.4%)	0.37 (0.15–0.96)	174% (128%–221%)
	HNG	NR	NR	NR	NR	NR	NR
14 DIV	HN	0.51 (0.39–0.67)	772% (712%–831%)	0.30 (0.16–0.54)	65.5% (53.8%–77.3%)	0.73 (0.64–0.83)	893% (853%–933%)
	HNG	NR	NR	0.80 (0.29–2.10)	50.2% (34.5%–66.8%)	1.29 (0.72–2.30)	83.3% (63.2–103.3%)

NR: No response

ND: Not determined